Chemical Engineering Journal Advances 8 (2021) 100180

Contents lists available at ScienceDirect

Chemical Engineering Journal Advances

journal homepage: www.sciencedirect.com/journal/chemical-engineering-journal-advances

Influence of counterdiffusion effects on mass transfer coefficients in stirred tank reactors

S. Matthes, T. Merbach, J. Fitschen, M. Hoffmann, M. Schlüter *

Institute of Multiphase Flows, Hamburg University of Technology, Germany

ARTICLE INFO

Keywords:
Counterdiffusion effects
Mass transfer coefficients
Stirred tank reactor
Micro sparger and conventional aeration
Fine bubbles
Degassing techniques

ABSTRACT

Accurate knowledge of volumetric oxygen mass transfer coefficients in multiphase systems is important for successfully designing and efficient operation of process plants. As a result, a large number of papers on the determination of volumetric mass transfer coefficients k_La have been published in the literature. The dynamic degassing method is probably the most common method for determining the volumetric mass transfer coefficient. However, little work is known on the influence of countercurrent diffusion effects, arising from further dissolved components, on the volumetric mass transfer coefficient.

For this reason, the effect of countercurrent diffusion is investigated in the present work by using different stripping gases to determine the volumetric oxygen mass transfer coefficient. Furthermore, the effect of counterdiffusion is investigated for both conventional aeration and aeration with microbubbles.

The present work shows that the choice of stripping gas has a decisive influence on the determination of the volumetric oxygen mass transfer coefficient. Moreover, it can be shown that this effect is directly proportional to the solubility of the stripping gas in the aqueous phase. Simultaneous measurements of bubble size distributions allow determining mass transfer coefficients k_L. A model is developed describing the decrease in the mass transfer coefficient as a function of the solubility of the stripping gas.

Furthermore, it can be shown that for the experimental determination of volumetric oxygen mass transfer coefficients, the choice of stripping gas should be adapted to secondary gas types occurring within real processes achieving a better comparability.

1. Introduction

In today's process industry the efficient supply of oxygen as an oxidant is a central part for various kinds of applications [1,2]. To utilize oxygen for a process the gas has to be dissolved in the liquid reaction medium. This is mostly done by aeration of the medium where the oxygen is provided by mass transfer across gas-liquid interfaces in multiphase contact apparatuses. The optimization of these complex two-phase reactor systems is still of high interest in terms of saving resources as well as enhancing yields. Due to the low solubility of oxygen in aqueous liquids at ambient conditions, achieving high mass transfer rates is mostly the bottleneck for high process efficiencies. By aeration with air as commonly applied in industry, the oxygen solubility is less than 0.5 % compared to the solubility of CO_2 which is a common side product to deal with in many processes [3–5]. Therefore, the measurement and prediction of mass transfer coefficients is a crucial task with regard to the design and scale-up of those systems. In process industry usually simplified model systems (water-air at ambient pressure) are used during the characterization of a process, reducing costs as well as the complexity. Two main aspects have to be taken into account by transferring the results to the real reactive system: Firstly, special treatments of the reaction media, such as degassing or addition of certain chemicals, are necessary for the measurements of mass transfer coefficients, having an influence on the resulting values. Secondly, within the real process side products occur (for example, in biotechnology: CO_2 during fermentations or in chemical processes: side products of a reaction) which are not considered in model systems. Especially the presence of further gases being dissolved in the liquid phase influences the mass transfer characteristics of a gas-liquid system. Gases with a higher solubility than the process gas (often oxygen is used) like CO_2 or argon have a negative influence on the dissolution rate of the process gas. Beside the mass transfer from the gaseous phase into the liquid, also countercurrent mass transfer of all dissolved gases into the

* Corresponding author.
E-mail address: michael.schlueter@tuhh.de (M. Schlüter).
URL: http://www.tuhh.de/ims (M. Schlüter).

https://doi.org/10.1016/j.ceja.2021.100180
Received 5 July 2021; Received in revised form 31 August 2021; Accepted 5 September 2021
Available online 6 September 2021
2666-8211/© 2021 The Authors. Published by Elsevier B.V. This is an open access article under the CC BY-NC-ND license (http://creativecommons.org/licenses/by-nc-nd/4.0/).

Nomenclature

Symbols

ν	kinematic viscosity, $m^2 \cdot s^{-1}$
ρ	density, $kg \cdot m^{-3}$
σ	surface tension, $N \cdot m^{-1}$
c	concentration, $mol \cdot L^{-1}$
c^*	saturation concentration, $mol \cdot L^{-1}$
D	diffusion coefficient, $m^2 \cdot s^{-1}$
d	diameter, m
d_{32}	Sauter diameter, m
d_{50}	arithmetic mean diameter, m
D_R	reactor diameter, m
h	height, m
H_R	reactor height, m
k_L	mass transfer coefficients, $m \cdot s^{-1}$
$k_L a$	volumetric mass transfer coefficient, s^{-1}
M	torque, N·m
P	power, W
S	solubility, $kg \cdot m^{-3}$
T	temperature, K
t	time, s
V	volume, m^3
a	fitting parameter, -
b	fitting parameter, -

Sub and Superscripts

B	bubble
fill	filling value
G	gas phase
L	liquid phase,
O	orifice
S	stirrer

Abbreviations

BSD	bubble size distribution
CMC	critical micelle concentration
DI	deionized
STR	stirred tank reactor

gaseous phase occurs. So far, there is a lack of knowledge considering the impact of this bidirectionality on the measurement of mass transfer coefficients. This work provides first results quantifying the decrease in the volumetric mass transfer coefficient $k_L a$ in dependence of the additionally dissolved gaseous component. Furthermore, the sensitivity of this counterdiffusion effect to the bubble size is analyzed.

2. Theoretical principles

For the characterization and scale-up of mass transfer limited processes precise information about the mass transfer efficiency of gas-liquid systems are required. Therefore, laboratory scale reactors are used determining volumetric mass transfer coefficients to evaluate the mass transfer performance of a gaseous components into the liquid phase. For various applications such as fermentation processes, oxygen has to be supplied for the reaction as an oxidant. Due to its common application and relevance for the process industry, this work focuses on the oxygen mass transfer from air into aqueous liquids and the influence of further dissolved gases in the liquid phase. For measuring volumetric oxygen mass transfer coefficients different methods can be used. One often in industry applied procedure is the oxygen balance method using a sulfite oxidation [6]. This method is characterized by its high accuracy and the possibility of measuring fast mass transfer processes with k_{La} values in the magnitude of several s^{-1}. One disadvantage is given by the high complexity as well as the required precision in the adjustment of the sulfite oxidation. For less fast mass transfer processes the dynamic method is commonly used, monitoring the increasing oxygen concentration during the aeration [7–10]. Utilizing this technique, a crucial task is the degassing of the liquid phase. The dissolved oxygen within the liquid phase has to be removed prior to each measurement. This is necessary analyzing the increasing dissolved oxygen concentration during aeration as described in Section 2.2. For the removal of dissolved oxygen physical as well as chemical approaches can be used [11]. The lowest dissolved oxygen concentrations are reached by chemical methods reducing the oxygen during a chemical reaction. Therefore, reducing agents such as sodium sulphite or hydrazine have to be added to the system [12]. The reducing agents are taking the effect of contaminants influencing the liquid system and its properties. Also, the needed reducing agent often has a toxic effect making it not suitable for all applications. The reducing agents can influence the liquid properties by changing the pH value of the system which can not be tolerated e.g. for enzymatic reactions. For this reason chemical methods are less applicable within the determination of mass transfer coefficients for the fundamental characterization of the mass transfer behavior of gas-liquid systems. In this case physical methods which do not lead to changes in the physiochemical properties of the system are preferable. Established and well examined techniques for the reduction of the dissolved oxygen content in aqueous liquids are boiling, pressure reduction or the aeration with inert gases like nitrogen [13]. Boiling as well as vacuum treatment of a liquid drive out all dissolved components, generating a pure system for the mass transfer measurements. Though, the experimental realization of those methods is challenging especially for large liquid volumes. Most commonly, the stripping of the system with nitrogen is used due to its easy handling and applicability to various setups. At the end of the stripping procedure, the dissolved oxygen is removed and nitrogen remains dissolved in the liquid phase. In this work the influence of different physical degassing methods on the measurements of volumetric mass transfer coefficients $k_L a$ is analyzed in a stirred vessel for different bubble sizes, ranging from micrometer to millimeter scale. The fundamental mass transfer characteristics of bubbly flows being elementary for the interpretation of the results are explained in the following.

2.1. Mass transfer in bubbly flows

According to the film theory of Lewis and Whitmann [14] the mass transfer of a component between two-phases is driven by a concentration gradient Δc. In an ideal gas-liquid system, only the mass transfer from the gaseous into the liquid phase is considered, due to the absence of further dissolved components. The mass transfer process is completed by reaching the maximum saturation concentration of the gas within the liquid as a function of pressure and temperature. For real systems the complexity of the mass transfer processes increases. Components of the fermentation media within the liquid get adsorbed at the gas-liquid interface resulting in a shielding effect which leads to reduced mass transfer rates. Also, further dissolved gases are often present in those systems. Living organisms produce substances like carbon dioxide, ethanol or methanol during their metabolic processes. A huge problem arises from the production of CO_2 by animal cells like CHO cells or bacteria like E. coli due to its high solubility and its influence on the pH value of the system. In this case, not only mass transfer from the gaseous phase into the liquid phase takes place, but also further dissolved components get desorbed into the bubbles. This counterdiffusion influences the mass transfer rate measured for the provided process gas

and takes place until all concentration gradients within the system are balanced. For a single free rising bubble, Hosoda et al. [15] first quantified the impact of countercurrent mass transfer in a gas-liquid system, investigating different bubble shapes depending on the diameter of the vertical channel in the experimental setup. They provide a model for calculating the bubble diameter during the dissolution process of a pure CO_2 bubble rising in air saturated water. Measurements of the gas compositions within the bubbles during their dissolution processes show the decreasing CO_2 concentration as well as the simultaneous increase of the N_2 and O_2 concentrations. Reaching an equilibrium state, the gas composition as well as the bubble diameter remain constant. Merker et al. observe the same behavior for a CO_2 bubble in nitrogen stripped water and point out the drastical changes in calculating the occurring mass transfer coefficients [16]. The effect of counterdiffusion influencing mass transfer rates is also visible considering the overall mass transfer coefficient of an aerated system. Muroyama et al. [17] investigated volumetric mass transfer coefficients in a bubble column reactor, using two different aeration techniques: one generating microbubbles and another for the formation of bubbles at the millimeter scale. In the microbubble aerated system, for completely degassed water up to twice the k_La values than for nitrogen-desorbed water are reached. In contrast to this, for bubbles larger than 2 mm there is no difference in the k_La values visible regarding the degassing method. In bubble swarms, the influence of counterdiffusion on mass transfer coefficients shows a strong dependence on the bubble size, which can be explained by the special mass transfer characteristics at the microscale. As pointed out so far, the mass transfer mechanisms for small scale bubbles differ from conventional theories [18]. Due to the acting surface tension, at microscopic scale the Laplace pressure influences the mass transfer by its direct impact on the saturation concentration given by Henry's law. Therefore, a changing bubble diameter has an impact on the mass transfer rate. As pointed out by Worden and Bredwell, in a gas mixture the amount of an insoluble component that influences the partial pressure of the oxygen and the shrinking rate of the bubble has to be taken into account [19,20]. Iwakiri et al. have visualized first this influence by comparing the shrinking rate of a single oxygen microbubble in vacuum treated water and nitrogen stripped water [21]. Having a high concentration of dissolved nitrogen in the water not only oxygen from the bubble is transferred into the liquid but at the same time nitrogen diffuses into the bubble reducing the shrinking rate of the microbubble as previously discussed.

This study focuses on the complex mass transfer mechanisms in bubble swarms considering countercurrent mass transfer due to the presence of different gases being dissolved in the liquid phase. A wide range of bubble sizes from the micrometer to the millimeter scale is analyzed in order to quantify the sensitivity of the volumetric mass transfer coefficient by gas desorption.

2.2. Experimental method

The influence of various dissolved gases on the mass transfer coefficients due to counterdiffusion effects is analyzed using a cylindrical lab scale stirred tank reactor with a flat bottom. The aerated stirred tank reactor (STR) has a diameter of $D_R = 105$ mm, a height of $H_R = 300$ mm and is equipped with three baffles. The reactor is placed in a cuboid basin to control the liquid temperature to $T = 25$ °C as well as to compensate optical distortion due to the curvature of the reactor using refractive index matching. To reduce the friction and to ensure optimal stability the stirrer shaft is fixed in the centre of the reactor lid using ceramic ball-bearings. The stirrer is driven by a ViscoPakt-rheo - X7 by HiTec Zang GmbH, Germany, which additionally measures the afforded torque with a resolution of $M_{res} = 0.003$ Ncm and a reproducibility of $M_{rep} = 0.05$ Ncm. For the agitation a single Rushton turbine with an impeller diameter of $d_S = 54$ mm is mounted at a bottom clearance of $h/d_S = 1$. For all experiments the liquid volume is $V_{fill} = 2$ L. Deionized (DI) water with 0.24 mmol/L Triton X-100 and pressurized air are used as material system. The standard surfactant Triton X-100 is added to the DI water to reduce the surface tension to $\sigma = 39.2$ mN/m presenting real biochemical systems as well as to achieve reproducible conditions. Volumetric power inputs in the range of $P{\cdot}V^{-1} = 40 - 640$ W/m^3 are analyzed representing shear sensitive biotechnical processes.

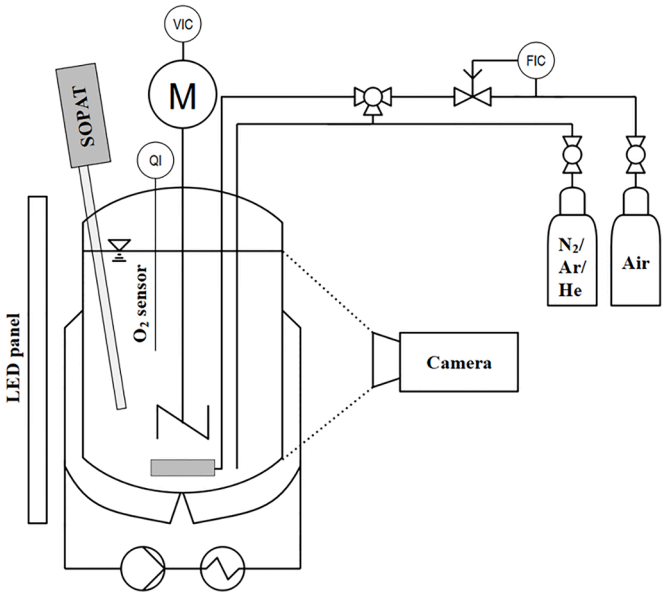

Fig. 1. Piping and instrumentation diagram of the STR setup.

As pointed out so far for fine bubbles, additional gases being present in the system strongly influence the mass transfer behavior due to simultaneous counterdiffusion [17,19,21]. To quantify the impact of those counterdiffusion effects for a large range of bubble sizes a micro sparger as well as a conventional open tube sparger with an orifice diameter of $d_O = 4$ mm is used. The micro sparger consists of a 316L stainless steel sintered frit with a mean pore size of 0.5 µm producing a high fine bubble density of bubbles smaller than $d_B = 100$ µm.

As visualized in Fig. 1, BSD are measured optically inside the bubbly flow using an endoscopic system SOPAT Sc by SOPAT GmbH, Germany and also from outside of the reactor. In this case, pictures are taken with an Optronis high-speed camera with a resolution of 450 x 450 pixels and a frame rate of 100 fps. For the illumination a LED panel is installed behind the reactor at the opposite side of the camera. A Matlab based bubble detection algorithm is used determining size and number of the bubbles.

For an evaluation of the mass transfer performance the volumetric mass transfer coefficient k_La is determined by the dynamic degassing method. Therefore, the dissolved oxygen is removed from the liquid phase reaching an initial dissolved oxygen concentration below 10% of the atmospheric oxygen saturation level. Subsequently, the aeration with air is started and the increase of the dissolved oxygen concentration c_{O_2} is recorded [22]. Pressurized air is used for the aeration and the gassing rate is held constant by a flow controller (Bronkhorst L-Flow). The k_La value is calculated according to

$$k_La = \frac{dc_{O_2}}{dt} \cdot \frac{1}{(c^* - c_{O_2})} \tag{1}$$

with the saturation concentration c^* and the measured oxygen concentration c_{O_2} at its corresponding time t. The saturation concentration c^* is measured for each gas-liquid system prior to the k_La measurements by aeration until equilibrium is reached. For the measurement of the dissolved oxygen concentration the optical oxygen probe FDO 925 (measurement range 0 to 200% DO saturation, accuracy 0.1% of saturation value, response time (t90) < 30 sec) by WTW, Germany is used. The stripping with nitrogen to remove the dissolved oxygen from the liquid

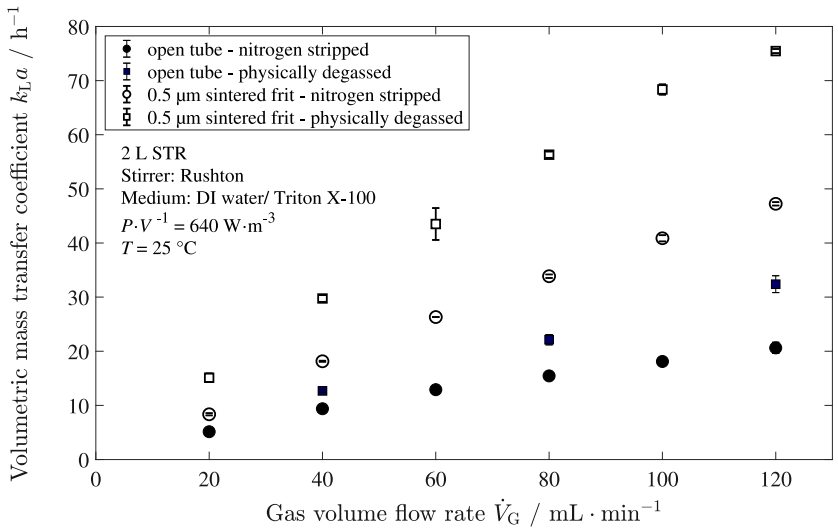

Fig. 2. Influence of the degassing method on the volumetric oxygen mass transfer coefficient for fine bubble aerated STR and conventional aerated STR.

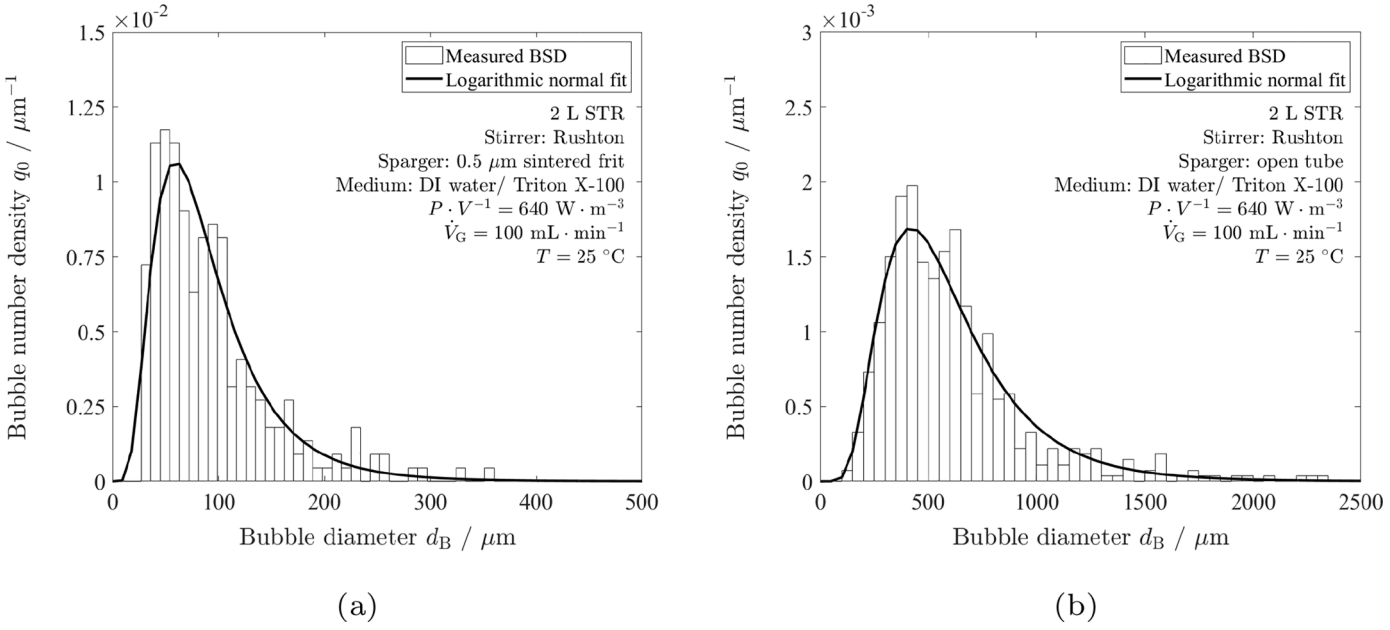

Fig. 3. Comparison of the BSD for sintered frit (a) and open tube (b) in the Triton X-100 system for $P{\cdot}V^{-1}$ = 640 W/m^3 and $\dot{V}_G$ = 100 mL/min.

is a well established procedure in process engineering. Besides nitrogen, also argon and helium are used for the stripping to analyze the influence of the stripping gas on the measured mass transfer coefficients. All gases have a different solubility S in water as given in Table 1. Therefore, after the stripping process the concentration of the stripping gas which gets dissolved in the water has a different level depending on its solubility. To enable a comparison with a system without any dissolved gases where no counterdiffusion takes place, the liquid is also degassed physically. Therefore, the liquid is boiled for several minutes to drive out all dissolved gases. In an airtight container the medium is cooled down to the operating temperature of T = 25 °C before it is decanted back to the reactor.

3. Results and discussion

To analyze the impact of different degassing methods on the measurement of mass transfer coefficients different bubble regimes are investigated. A novel micro sparger as well as a conventional open tube sparger is used, covering a wide bubble range from several micrometers to a few millimeters. The microbubble aeration enables generating a narrow BSD below 100 µm. As illustrated in Fig. 2, for a fixed power input of $P{\cdot}V^{-1}$ = 640 W/m^3, the fine bubble aerated system reaches higher volumetric mass transfer coefficients than the conventional aerated system independent of the air volume flow rate. The benefit of fine bubble aeration due to higher interfacial areas and a mass transfer enhancing effect of the Laplace pressure is described in detail by Matthes et al. [18]. Regarding the influence of the degassing method, stripping with nitrogen is used as reference. This approach is most common due to an easy handling and the low costs of the stripping gas. For both spargers, the physically degassed system reaches up to 1.8 times higher mass transfer coefficients compared to the nitrogen stripped system due to the lack of counterdiffusion. The reduction of the k_La due to counterdiffusion of the dissolved nitrogen is more pronounced for the micro sparger producing fine bubbles than for the conventional aerated system.

Due to the influence of the counterdiffusion on the partial pressure of

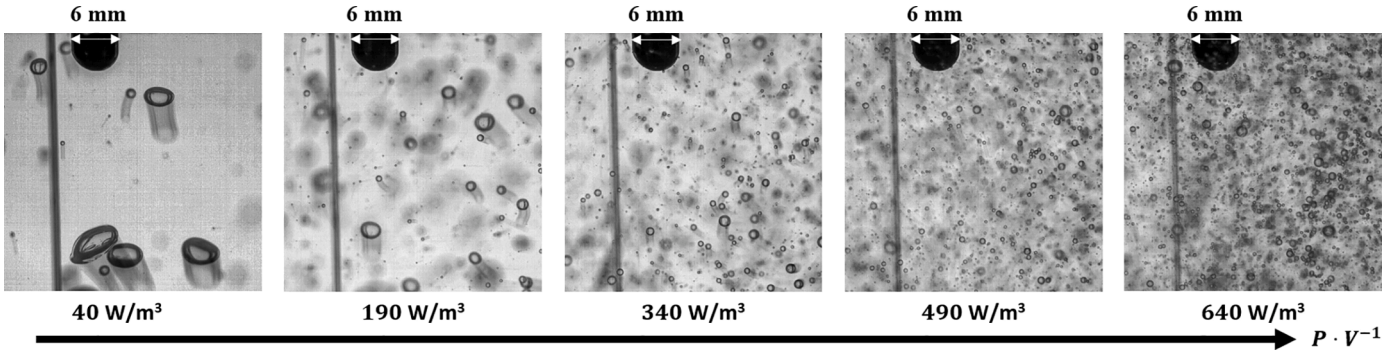

Fig. 4. Snapshots of bubble sizes in conventional aerated STR (open tube sparger) in dependence of the power input.

Table 1
Literature values for the solubility of the stripping gases and oxygen in water at $T = 25$ °C [23].

Gas	Solubility S / mg·L^{-1}
Helium	1.5
Nitrogen	17.5
Argon	53.0
Oxygen	8.2

Table 2
Arithmetic mean diameter and Sauter diameter for the open tube aerated system for various power inputs.

Vol. power input $P{\cdot}V^{-1}$ / W·m^{-3}	Arithmetic mean diameter d_{50} / µm	Sauter diameter d_{32} / µm
40	930	5005
190	751	2244
340	580	1028
490	437	786
640	394	484

the oxygen within the bubble, the initial bubble size in the system is important for the impact on the mass transfer. For larger bubbles the counterdiffusion has less influence on the mass transfer rate due to a smaller impact of the Laplace pressure on the total pressure inside the bubble. Additionally, the amount of gas transferred into the bubble is negligibly small to the total volume of the bubble.

Comparing the BSD for both spargers according to Fig. 3, it is visible that the open tube creates 10 times larger bubbles compared to the micro sparger. The bubble sizes are logarithmic normal distributed for both spargers. The modal value for the BSD of the micro sparger is given by $d_B = 50$ µm while for the open tube its value is at around $d_B = 500$ µm. The larger bubbles in the system with the open tube sparger point out the importance of the bubble size on the impact of the counter-diffusion effect. But, still for the larger bubble sizes in the conventional aerated system, the volumetric mass transfer coefficients measured by the most frequently applied gas stripping method with nitrogen are nearly 50% smaller than the reference values obtained from the physically degassed system regarding the analyzed power input of $P{\cdot}V^{-1} = 640$ W/m^3.

For a better quantification of the influence of bubble size and bubble shape on the counterdiffusion effect, the conventional aerated STR setup is further investigated. The mass transfer coefficient is determined for all stripping gases (helium, nitrogen and argon) and the physically degassing method applying different volumetric power inputs reaching from $P{\cdot}V^{-1} = 40$ W/m^3 to $P{\cdot}V^{-1} = 640$ W/m^3. As displayed in Fig. 4, for the open tube sparger the bubble size and shape strongly depends on the power input. For a small power input of $P{\cdot}V^{-1} = 40$ W/m^3, shape oscillating bubbles of a few millimeter are generated. With increasing power input the bubbles become smaller and more spherical.

The changing mean diameters of the bubbles within the conventional aerated stirred tank reactor are given in Table 2 for all investigated power inputs.

Figure 5 shows the results for the mass transfer measurements in the open tube setup for all power inputs and degassing methods. In general the volume specific mass transfer coefficient increases with increasing power input due to the above described reduction in the bubble size and the resulting increase in the volume specific interfacial area.

For the lowest power input where the bubbles appear shape oscil-

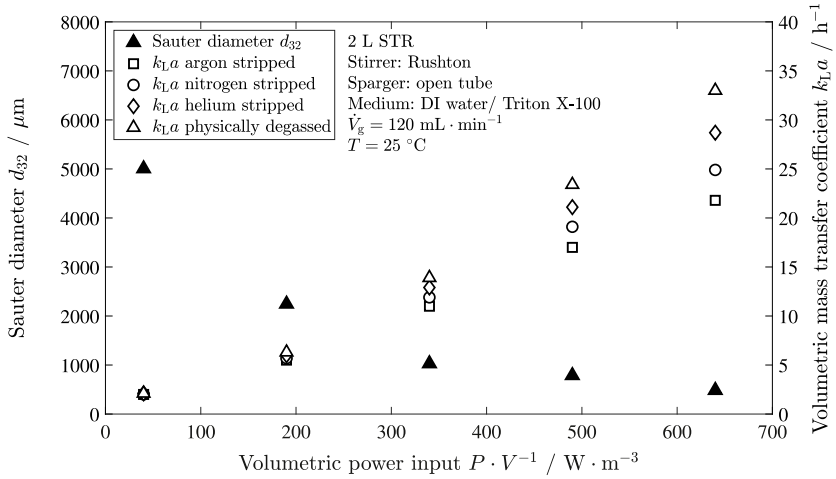

Fig. 5. Volume specific mass transfer coefficients and Sauter diameter for conventional aerated STR as a function of the power input and the degassing method.

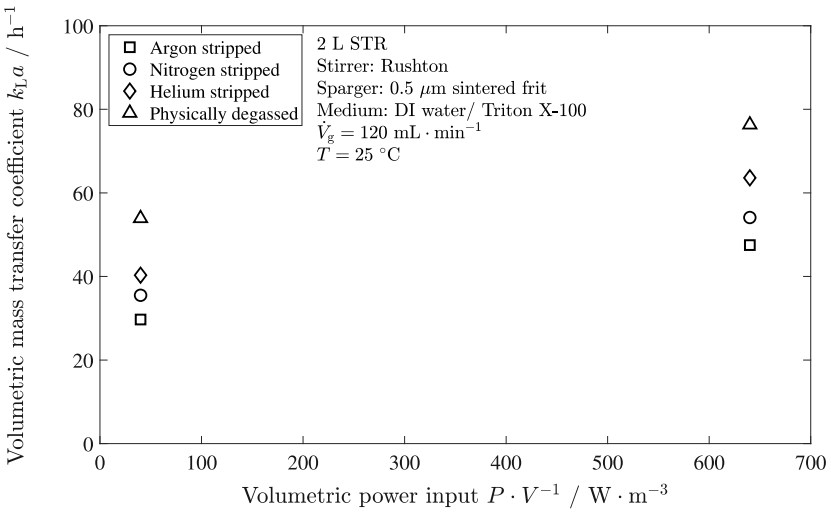

Fig. 6. Volume specific mass transfer coefficients for membrane aerated STR as a function of the power input and the degassing method.

Table 3
Sauter diameter and volume specific mass transfer coefficient for different degassing methods for fine bubble aerated system at $P{\cdot}V^{-1} = 40$ W/m^3.

Degassing method	Vol mass transfer coefficient k_La / h^{-1}	Sauter diameter d_{32} / µm
Physically degassed	53.85	271
Helium stripped	40.30	279
Nitrogen stripped	35.51	286
Argon stripped	29.67	310

lating, the measured k_La values are equal for all degassing methods. Due to the larger bubble volume, the amount of the stripping gas that is transferred into the bubble does not lead to a significant change of the total bubble volume and its diameter. Also, the changing Laplace pressure has no significant influence on the total pressure inside the bubble for this large dimensions. Therefore, the partial pressure of the oxygen remains nearly constant. Furthermore, for large oscillating bubbles the deformation of the bubble surface is the dominating effect driving the mass transfer as described by Timmermann [24] and not the Laplace pressure as pointed out for fine bubbles [18,21].

Without occurring bubble deformations and with decreasing bubble size the influence of the stripping method gets visible. For a mean Sauter diameter smaller than $d_{32} \approx 1000$ µm there are significant differences in the measured k_La values due to the counterdiffusion of the stripping gas. At this point the amount of stripping gas diffusing into the bubble is large enough compared to its initial volume to change the composition of the gas mixture inside the bubble. The oxygen gets diluted and its partial pressure decreases. The highest k_La values are reached for the physically degassed system and with increasing solubility of the stripping gas the k_La values are decreasing. The higher the solubility of the stripping gas the more of it gets dissolved during the stripping process. As a result, there is a strong concentration gradient for the stripping gas from the water towards the bubble that correlates with the amount of gas diffusing into the bubble.

For fine bubble aeration, the bubble size is primary determined by the geometry of the sparger and dispersion mechanisms leading to smaller bubbles due to the stirrer are negligible [18]. The micro sparger used within this study is producing a narrow BSD with $d_{32} \leq 1000$ µm independent of the power induced by the stirrer. Therefore, for the micro sparger the influence of the counterdiffusion on the k_La values is visible for the smallest as well as for the largest power input as shown in Fig. 6.

For the micro sparger, simultaneous BSD measurements of the fine bubble flow and the volume specific mass transfer coefficient are done to show the influence of the degassing method and the bubble sizes on the mass transfer performance. A comparison of the Sauter diameters for the four degassing methods, as given in Table 3, allows a conclusion of the amount of stripping gas that is transferred into the bubble. Comparing the measured volumetric mass transfer coefficients with the Sauter mean diameters that are measured during aeration, it can be seen that the physically degassed system has the lowest Sauter diameter. With increasing solubility of the stripping gas, as well as a higher influence of counterdiffusion, the Sauter diameter of the dispersed gas phase increases. The more gas is diffused into the bubble, the lower gets the partial pressure of the oxygen and therefore the oxygen saturation concentration at the interface. The mass transfer of the dissolved component into the bubble and the oxygen from the bubble into the liquid phase proceed simultaneously. The amount of dissolved gas being absorbed by the bubbles is significantly smaller due to the smaller volume of the gas phase compared to the liquid phase combined with the low gas hold-up. Therefore, the counterdiffusion process is completed much faster compared to the oxygen mass transfer. Thus, the complexity of the system can be simplified by considering the oxygen mass transfer separately after the completed counterdission process. So the different mass transfer performances are equal to the one which are observed for different initial gas mixtures presented by Worden and Bredwell [19]. The validity of this simplification gets confirmed by the continuously increasing oxygen concentration profiles measured during the aeration having no discontinuities. The end of the counterdiffusion process in middle of the oxygen transfer would lead to an increased oxygen transfer rate being visible in the concentration profile due to an lower mass transfer resistence.

For microscopic bubbles additionally the influence of the Laplace pressure on the partial pressure of the oxygen has to be taken into account, which is decreasing with increasing bubble size. As a result, in a fine bubble aerated system for each bubble size, a specific saturation concentration has to be defined for a correct description of the mass transfer according to the film theory. Experimentally, only global dissolved oxygen concentrations are measured and the global saturation concentration of the water/air system is determined. The global saturation concentration of the system remains constant as given by Henry's law. Due to the strong influence of the Laplace pressure on the partial pressure of the oxygen, local deviations in the saturation concentration at the interfaces of the bubbles occur. These deviations cannot be covered in the measurements and are therefore not taken into account for the calculations of the mass transfer coefficients. Thus, the oxygen diffusion coefficient gets apparently reduced, resulting in smaller k_L values calculated from the measurements.

Table 4
Mass transfer coefficient for different degassing methods obtained in fine bubble aerated STR system.

Degassing method	Mass transfer coefficient k_L / m·h^{-1}	Measurement deviation Δk_L / m·h^{-1}
Physically degassed	1.05	±0.079
Helium stripped	0.9	±0.054
Nitrogen stripped	0.74	±0.101
Argon stripped	0.67	±0.094

In Table 4, the k_L values calculated from the mass transfer measurements in the fine bubble aerated Triton X-100 system (results given in Fig. 6) according to

$$a = 6 \cdot \frac{\varepsilon_G}{d_{32}} \tag{2}$$

are shown. The Sauter mean diameter is given by the measured BSD. For the determination of the corresponding volume specific interfacial area, the gas hold-up has been determined using the images taken by the SOPAT probe following the procedure explained by Matthes et al. [18].

To include the influence of the stripping gas on the obtained mass transfer coefficients, a model is developed using dimensionless analysis which includes the dependence between the solubility of the stripping gas and the overall calculated mass transfer coefficient. As a reference, the physically degassed system ($k_L = k_{L,0}$) is used. Fig. 7 displays the defined dependency which is described by a fractional-rational function of the form

$$\frac{k_L}{k_{L,0}} = \frac{a \cdot D_{O_2} \cdot S \cdot \nu_L^{-1} + b \cdot \rho_L}{S + b \cdot \rho} \tag{3}$$

with the substance data D_{O_2}, ρ_L, ν_L and the solubility S of the stripping gas as variable parameter. The shape of the correlation is defined as fractional-rational function using the Matlab based curve fitting toolbox. The exact form of Eq. (3) and the influencing substance data is determined by dimensional analysis. For the analyzed fine bubble aerated 2 L STR setup with an aqueous solution of the standard surfactant Triton X-100 at its critical micelle concentration (CMC), the fitting parameter a and b are defined as $a = 2.7 \cdot 10^2$ and $b = 2.7 \cdot 10^{-6}$. Reaching the CMC results in a saturation of the complete interface with the surfactant, ensuring uniform and reproducible conditions for the mass transfer process. The developed correlation enables the conversion of the mass transfer coefficient between the different stripping methods, characterized by the solubility of the stripping gas.

The results of the counterdiffusion experiments presented in this section point out how important it is to capture all components that are present in the system. For fermentation processes for example gases like carbon dioxide are generated during the process which influences the overall mass transfer. The information on the counterdiffusion can help to modify mass transfer measurements during the design of a process so that the real process is better predictable and can thus be reproduced more accurately. Good knowledge of the considered process will help reproducing its mass transfer behavior in a model system. A side product that is produced during the real process and its influence on the mass transfer rate can be simulated using a stripping gas with a similar solubility. For real fermentation processes the volumetric mass transfer coefficient is a good basis for the scale-up of the system. A better conformity of the k_La values between the different systems will lead to more accurate results in the scale-up process.

4. Summary

The measurement of mass transfer coefficients is a crucial aspect for characterizing multiphase systems. Especially for mass transfer limited systems, the correct determination of mass transfer rates within the process design is necessary to achieve the highest efficiencies. Therefore, all aspects influencing the mass transfer between the gas and the liquid phase have to be taken into account. Within this study, the impact of counterdiffusion effects, leading to reduced mass transfer rates, is experimentally analyzed for bubble swarms with gas hold-ups of up to 1 %. The investigation of different bubble sizes and shapes points out that below a critical characteristic bubble diameter of $d_{32} \leq 1000$ µm the influence of counterdiffusion can no longer be neglected. The influence of the degassing method on measured mass transfer coefficients is quantified by comparing different commonly used physical degassing methods: boiling as well as gas stripping with argon, nitrogen or helium. In combination with the knowledge of the bubble size distribution during the mass transfer process, a novel model is introduced. It allows calculating mass transfer coefficients, considering the solubility of the stripping gas. The developed model should be implemented into process simulations, so that in the future, real systems can be considered capturing the influence of all substances on the mass transfer rates, i.e. the mass transfer coefficients. In a next step, the applicability of the model for the scale-up of reactor systems has to be considered, taking into account the impact of bubble size and gas hold-up on the mass transfer process. Furthermore, the influence other dissolved gases as

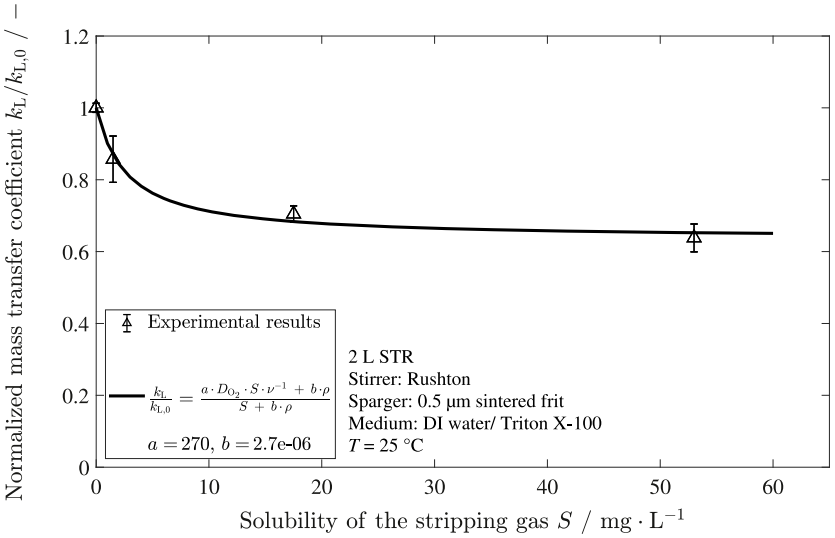

Fig. 7. Correlation of the mass transfer coefficient as a function of the solubility of the stripping gas as given in Table 1.

well as mass transfer limited reactive systems are of interest to extend the field of application.

Declaration of Competing Interest

The authors declare that they have no known competing financial interests or personal relationships that could have appeared to influence the work reported in this paper.

Acknowledgements

The authors gratefully express their gratitude to the German Research Foundation (DFG) for the financial support within the project SCHL 617/14-1. Especially we would like to thank Prof. Koichi Terasaka from Keio University as Mercator Fellow providing his profound knowledge in fine bubble technology.

References

[1] M. Bothe, Experimental Analysis and Modeling of Industrial Two-Phase Flows in Bubble Column Reactors, Dissertation at Hamburg University of Technology volume 1, Cuvillier Verlag, 2016.
[2] B. Thomas, D. Ohde, S. Matthes, C. Engelmann, P. Bubenheim, K. Terasaka, M. Schlüter, A. Liese, Comparative investigation of fine bubble and macrobubble aeration on gas utility and biotransformation productivity, Biotechnol. Bioeng. (2020).
[3] L. Chu, D.K. Robinson, Industrial choices for protein production by large-scale cell culture, Curr. Opin. Biotechnol. 12 (2) (2001) 180–187.
[4] A.W. Nienow, Reactor engineering in large scale animal cell culture, Cytotechnology 50 (1–3) (2006) 9.
[5] C. Sieblist, O. Hägeholz, M. Aehle, M. Jenzsch, M. Pohlscheidt, A. Lübbert, Insights into large-scale cell-culture reactors: II. Gas-phase mixing and CO2 stripping, Biotechnol. J. 6 (12) (2011) 1547–1556.
[6] E.R. Flores, F. Perez, M. De la Torre, Scale-up of Bacillus thuringiensis fermentation based on oxygen transfer, J. Ferment. Bioeng. 83 (6) (1997) 561–564.
[7] F. García-Ochoa, E. Gómez, Mass transfer coefficient in stirred tank reactors for xanthan gum solutions, Biochem. Eng. J. 1 (1) (1998) 1–10.
[8] A. Sánchez Mirón, F. García Camacho, A. Contreras Gómez, E.M. Grima, Y. Chisti, Bubble-column and airlift photobioreactors for algal culture, AlChE J. 46 (9) (2000) 1872–1887.
[9] M.S. Puthli, V.K. Rathod, A.B. Pandit, Gas–liquid mass transfer studies with triple impeller system on a laboratory scale bioreactor, Biochem. Eng. J. 23 (1) (2005) 25–30.
[10] H. Djelal, F. Larher, G. Martin, A. Amrane, Effect of the dissolved oxygen on the bioproduction of glycerol and ethanol by Hansenula anomala growing under salt stress conditions, J. Biotechnol. 125 (1) (2006) 95–103.
[11] F. Garcia-Ochoa, E. Gomez, Bioreactor scale-up and oxygen transfer rate in microbial processes: an overview, Biotechnol. Adv. 27 (2) (2009) 153–176.
[12] V. Sinha, K. Li, Alternative methods for dissolved oxygen removal from water: a comparative study, Desalination 127 (2) (2000) 155–164.
[13] I.B. Butler, M.A. Schoonen, D.T. Rickard, Removal of dissolved oxygen from water: a comparison of four common techniques, Talanta 41 (2) (1994) 211–215.
[14] W. Lewis, W. Whitman, Principles of gas absorption. Ind. Eng. Chem. 16 (12) (1924) 1215–1220.
[15] S. Hosoda, S. Abe, S. Hosokawa, A. Tomiyama, Mass transfer from a bubble in a vertical pipe, Int. J. Heat Mass Transf. 69 (2014) 215–222.
[16] D. Merker, L. Böhm, M. Oßberger, P. Klüfers, M. Kraume, Mass transfer in reactive bubbly flows–a single-bubble study, Chem. Eng. Technol. 40 (8) (2017) 1391–1399.
[17] K. Muroyama, K. Imai, Y. Oka, J. Hayashi, Mass transfer properties in a bubble column associated with micro-bubble dispersions, Chem. Eng. Sci. 100 (2013) 464–473.
[18] S. Matthes, B. Thomas, D. Ohde, M. Hoffmann, P. Bubenheim, A. Liese, S. Tanaka, K. Terasaka, M. Schlueter, Hydrodynamic and mass transfer correlation in a microbubble aerated stirred tank reactor, J. Chem. Eng. Jpn. 53 (10) (2020) 577–584.
[19] R.M. Worden, M.D. Bredwell, Mass-transfer properties of microbubbles. 2. Analysis using a dynamic model, Biotechnol. Prog. 14 (1) (1998) 39–46.
[20] M.D. Bredwell, R.M. Worden, Mass-transfer properties of microbubbles. 1. Experimental studies, Biotechnol. Prog. 14 (1) (1998) 31–38.
[21] M. Iwakiri, K. Terasaka, S. Fujioka, M. Schlueter, S. Kastens, S. Tanaka, Mass transfer from a shrinking single microbubble rising in water, Jpn. J. Multiphase Flow 30 (5) (2017) 529–535.
[22] A. Rosseburg, Influence of Heterogeneous Bubbly Flows on Mixing and Mass Transfer Performance in Stirred Tanks for Mammalian Cell Cultivation: A Study in Transparent 3 L and 12 000 L Reactors, Dissertation at Hamburg University of Technology vol. 5, Cuvillier Verlag, 2019.
[23] H. Baehr, K. Stephan, Heat and Mass Transfer, Springer-Verlag Berlin Heidelberg, 2011.
[24] J. Timmermann, Experimental Analysis of Fast Reactions in Gas-Liquid Flows, Dissertation at Hamburg University of Technology vol. 3, Cuvillier Verlag, 2018.